AN INTERPRETATION OF A FAR ULTRAVIOLET DAYGLOW EXPERIMENT

T. M. Donahue

(Planetary and Space Science)

University of Pittsburgh

Pittsburgh, Pennsylvania

October 15, 1965

AN INTERPRETATION OF A FAR ULTRAVIOLET DAYGLOW EXPERIMENT

T. M. Donahue

The University of Pittsburgh

Pittsburgh, Pennsylvania

(Received)

ABSTRACT

The altitude profile to 700 km of the OI 1302-06 dayglow brightness produced by resonance scattering of sunlight is calculated for the conditions prevailing at the time of Fastie's high altitude rocket experiment. The experimental results fit the calculated profile only above 550 km. Below there is an excess of radiation for which a primary excitation profile is calculated. The rate has a maximum of about 30 per cm^3 near 190 km. It is also sufficient with reasonable modifications to account completely for the excitation of the altitude profile of the 1356 line.

The altitude profile observed for the Lyman α line is shown to be consistent with a hydrogen abundance between 4 and 10 x 10^{13} atmos/cm^2 above 100 km and indicates a large increase in the hydrogen content of the atmosphere at solar minimum.

1. Calculation of the 1304 Dayglow Intensity

At an exospheric temperature of 850° the density of atomic oxygen as a function of altitude between 200 km and 700 km is given in Table 1. This model is designed to fit at 200 km the measurements of the Minnesota group[1]. The integrated abundance in atoms/cm^2 is also shown in the table for this model. To calculate the contribution of resonance scattering of the solar 1302-06 triplet to the overhead airglow intensity in these lines the method developed in previous papers[2, 3] is followed.

The solar lines are assumed to be flat topped with a full width of 0.2Å and to have the intensities 0.013 ergs/cm^2 sec (1302Å), 0.020 ergs/cm^2 sec (1304Å), and 0.025 ergs/cm^2 sec (1306Å)[4]. This radiation is assumed to be absorbed by oxygen atoms in the three ground state fine structure levels $^3P_2$, $^3P_1$ and $^3P_0$ exciting the 3s $^3S_1$ resonance level. Because of the 850° temperature above 200 km the oxygen atoms are distributed in the three levels with the fraction in one level being

$$p_i = \frac{g_i \, e^{-Ei/kT}}{\Sigma \, g_i \, e^{-Ei/kT}} \qquad (1)$$

The relative population of the $^3P_2$ level is 0.62, of the $^3P_1$ level is 0.29, and of the $^3P_0$ level is 0.08 at 850°.

Because of Doppler broadening the cross section for absorption varies with frequency as

$$\sigma_i(x) = \sigma_{oi} \, e^{-x^2} \qquad (2)$$

where $$x = \frac{\nu - \nu_o}{\Delta\nu_D} \qquad (3)$$

and at 850°

$$\Delta\nu_D = 0.72 \times 10^{10} \text{ sec}^{-1} \quad . \qquad (4)$$

Here

$$\sigma_{oi} = \frac{\pi e^2}{mC} \frac{f_i}{\sqrt{\pi}\Delta\nu_D} \qquad (5)$$

where f_i is the oscillator strength of the fine structure lines. All three values of f_i are approximately 0.30[5] and thus

$$\sigma_o \cong 5.8 \times 10^{-13} \text{ cm}^2 \qquad (6)$$

is the cross section for absorption at the central frequency of each line.

As was discussed in a previous paper[3] it is necessary to take account of absorption and radiation in the natural wings of these lines at altitudes below 200 km. For the purposes of this paper where the resonance radiation field at high altitude is at issue these effects are of secondary importance.

The optical thickness of the oxygen above an altitude z in any one line is

$$\tau_i = \sigma_{oi} \int_z^\infty n(z)\, dz \qquad (7)$$

Table 1 shows the optical thickness in the three lines from 200 km to 700 km. In the case being treated the sunlight is incident at a zenith angle of 60° so the optical thickness for absorption of solar radiation above any altitude is twice the value shown in the table or τ_i/μ where μ is the cosine of the solar zenith angle.

After the $^3S_1$ level is excited by absorption of a solar photon in any of the three lines re-radiation occurs in one of the three lines (not necessarily the one absorbed to excite the $^3S_1$ level). The branching ratios in the three lines which can be emitted is 5:3:1. The spectral distribution in a line again is Doppler shaped with a high probability of emission not farther from the line center than the absorbed photon was from the center of its line. This photon in turn can be absorbed and re-radiated again passing from atom to atom until it escapes upward or is absorbed below 110 km by an oxygen molecule .

The method of calculating the rate $j_i(\tau)$ at which the $^3S_1$ level is excited as a consequence of absorption of photons in the i^{th} solar line and subsequent multiple scattering is described in previous papers[2, 3]. This rate can be obtained separately for the contribution from each of the three solar lines as a function of the optical depth in the medium τ_i for that line. Each is got from a solution of the integral equation

$$j_i(\tau_i) = j_{oi}(\tau_i) + \int j_i(\tau_i') H(\tau_i, \tau_i') \, d\tau_i' \qquad (8)$$

where in the integral $j_i(\tau_i)$ is the emission rate and

$$H(\tau_i, \tau_i') = \frac{5}{9} H_5(\tau_i, \tau_i') + \frac{1}{3} H_3(\tau_i, \tau_i') + \frac{1}{9} H_1(\tau_i, \tau_i') \qquad (9)$$

Table 1

z km	n(0) cm^{-3}	τ_5 (1302)	τ_3 (1304)	τ_1 (1306)
120	5×10^{10}	3.3(4)	1.55(4)	4.3(3)
160	4.8×10^{9}	6.6(3)	3.1 (3)	8.6(2)
200	1.3×10^{9}	2.7(3)	1.26(3)	3.5(2)
250	4.4×10^{8}	8.1(2)	3.8 (2)	1.05(2)
300	1.6×10^{8}	3.0(2)	1.4 (2)	3.9 (1)
350	5.7×10^{7}	1.1(2)	5.4 (1)	1.5(1)
400	2.1×10^{7}	4.3(1)	2.0 (1)	5.5
450	8.0×10^{6}	1.65(1)	7.7	2.1
500	3.1×10^{6}	6.2	2.9	8(-1)
550	1.2×10^{6}	2.4	1.1	3.1(-1)
600	4.7×10^{5}	1.0	4.7(-1)	1.3(-1)
650	1.9×10^{5}	3.9(-1)	1.8(-1)	5(-2)
700	7.5×10^{4}	1.6(-1)	7.5(-2)	2(-2)

is the probability that a photon emitted between τ_i' and $\tau_i' + d\tau_i'$ will be captured per unit optical thickness at τ_i.* $j_{oi}(\tau_i)$ is the primary excitation rate given by

$$j_{oi}(\tau_i) = \pi F_{oi} \sqrt{\pi}(\Delta\nu_D/\Delta\nu_S) \; T(\tau_i) \tag{10}$$

where

$$T(\tau_i) = \frac{1}{\sqrt{\pi}} \int_0^{\tau_i} e^{-x^2} \, e^{-\tau_i e^{-x^2}} \, dx \tag{11}$$

is the transmission coefficient for resonance radiation in a Doppler shaped line. The three different values for the intensities of the solar lines give

$$\pi F_o(1302) \sqrt{\pi} \, \Delta\nu_D/\Delta\nu_S = 6.25 \times 10^7 \tag{12}$$

$$\pi F_o(1304) \sqrt{\pi} \, \Delta\nu_D/\Delta\nu_S = 9.7 \times 10^7 \tag{13}$$

and

$$\pi F_o(1306) \sqrt{\pi} \, \Delta\nu_D/\Delta\nu_S = 12.0 \times 10^7 \tag{14}$$

in units of photons/cm^2 sec.

---

*$H_K(\tau_i, \tau_i')$ per unit optical depth, τ_i, is $(p_k/p_i) \, H(\tau_i \, p_k/p_i)$ in terms of the kernel $H(\Delta\tau_K)$ for transfer of the kth line per unit τ_k, the increment in optical depth always being related to dz through

$$d\tau_i = p_i \, n(z) \, \sigma_o \, dz \tag{15}$$

The solution of the three transfer equations for the $j_i(\tau_i)$ will give the excitation rates in terms of three respective optical depths. To combine them it is first necessary to express them in terms of a single variable, say τ_5. This can be done by multiplying the rate per unit optical depth in λ1304 by p_3/p_5 or 0.47 and the rate per unit optical depth in λ1306 by p_1/p_5 or 0.13. The result is shown in Table 2.

The overhead brightness in each of the lines may be computed from the emission rates

$$4\pi I_5 = \frac{5}{9} \int_{\tau_5}^{\infty} j(\tau_5') \; T \; (\tau_5', \tau_5) \, d\tau_5 \tag{16}$$

$$4\pi I_3 = \frac{1}{3} \int_{\tau_3}^{\infty} j(\tau_3') \; T \; (\tau_3, \tau_3') \, d\tau_3' \tag{17}$$

$$4\pi I_1 = \frac{1}{9} \int_{\tau_1}^{\infty} j(\tau_1') \; T \; (\tau_1, \tau_1') \, d\tau_1' \tag{18}$$

The emission rates vary so slowly with altitude that a very good approximation to these integrals is

$$4\pi I_k = \frac{g_k}{\Sigma g_i} \; j(\tau_k) \int_{\tau_k}^{\infty} T(\tau_k') \, d\tau_k' \tag{19}$$

The integral in this expression is the equivalent width function

$$W(\tau) = \frac{1}{\sqrt{\pi}} \int_{-\infty}^{+\infty} \left[1 - \exp(-\tau e^{-x^2})\right] dx \tag{20}$$

Table 2

Altitude km	$J_5(\tau_5)$	$J_3(\tau_5)$	$J_1(\tau_5)$	$J(\tau_5)$	$J(\tau_3)$	$J(\tau_1)$
	in 10^9 photons/cm^2 sec per unit optical depth					
200	.145	.105	.035	.29	.62	2.24
250	.14	.10	.035	.27	.58	2.1
300	.125	.09	.03	.25	.53	1.9
350	.12	.09	.03	.24	.51	1.85
400	.12	.09	.03	.24	.51	1.85
450	.12	.09	.03	.24	.51	1.85
500	.12	.09	.03	.24	.51	1.85
550	.125	.09	.03	.25	.53	1.9
600	.13	.095	.03	.26	.56	2.0
650	.14	.1	.035	.27	.58	2.1
700	.14	.1	.035	.27	.58	2.1

which can be approximated for large and small τ by

$$\sum_{n=1}^{\infty} \frac{(-1)^{n+1} \tau^n}{n! \sqrt{n}} \qquad (21)$$

and

$$0.93 \sqrt{\ln \tau} \qquad (22)$$

respectively[5]. $W(\tau)$ varies rapidly for small τ and slowly for large τ. Thus

$$W(0.1) \cong 0.097$$
$$W(0.5) \cong 0.42$$
$$W(1) \cong 0.62$$
$$W(10) \cong 1.40$$
$$W(100) \cong 2.0$$
$$W(10^3) \cong 2.44$$
$$W(10^4) \cong 2.72$$

Integration gives for the three fine structure lines the values shown in Table 3.

To these must be added 90, 70 and 20 Rayleighs at 200 km and 30 5 and 2 Rayleighs at 250 km because of single scattering in the natural wings[3]. The three lines are thus 495, 545 and 555 Rayleighs in brightness at 200 km (1.6 kR combined) and 375, 415 and 445 R (1.23 kR in all) at 250 km.

Table 3

Altitude $4\pi I$ in Rayleighs

km	1302	1306	1304	Sum
200	405	535	490	1430
250	345	445	410	1200
300	300	375	355	1030
350	275	320	320	915
400	245	280	275	800
450	215	185	230	630
500	190	115	175	480
550	135	65	120	320
600	95	30	80	205
650	55	12	38	105
700	25	13	4	42

2. Calculation of the Excess Primary Excitation

A comparison of the theoretical curve with Fastie's experimental results is made in Fig. of the preceding paper. The combined experimental uncertainties in solar flux, line widths and shapes, and the dayglow absolute brightness render a comparison of absolute values impossible. The experimental curve in shape is asyntotic to the theoretical one, however, fitting it closely above 550 km. It rises much more steeply as the altidude decreases however. Compared to the case of absorption from flat topped solar lines an excess of photons is somehow being fed into the mechanism at low altitudes. As Fastie suggests these could come from the more intense wings of deeply reversed solar lines. They also could originate because of local excitation of atomic oxygen near 200 km. The primary excitation rate required can be determined by subtracting the resonance scattered solar contribution from the experimental brightness, unfolding the excess excitation rate $j'(\tau)$ and eventually obtaining the excess primary excitation rate $j_o'(\tau)$ by solving the equation

$$j_o'(\tau) = j(\tau) - \int j'(\tau') H(\tau,\tau') d\tau' \qquad (23)$$

Where $H(\tau,\tau')\, d\tau\, d\tau'$ is the probability that a photon emitted between τ' and $\tau' + d\tau'$ will be absorbed between τ and $\tau + d\tau$.

Assuming for the sake of calculating something that the radiative transfer calculation gives correctly the contribution of solar photons and normalizing the experimental data to this theoretical curve at peak altitude the excess intensity is obtained by subtraction. Below 240 km the experimental curve is assumed to follow the trend of previous measurements[2, 6] and the theoretical solar contribution to be given by our

previous calculation[3] which takes into account scattering in the natural wings of the lines and the variation in temperature. The excess radiation is plotted in Fig. 1 as a function of altitude. The rate of excitation $j'(\tau_5)$ necessary to produce this intensity is next calculated by solving

$$4\pi I'(\tau_5) = \int_0^{\tau_5} j'(\tau_5)\, T_{eff}(\tau_5, \tau_5')\, d\tau_5' \qquad (24)$$

for j'. In (24) it is necessary, particularly at high altitude, to use for the transmission function the weighted sum of the transmission functions for the three lines

$$T_{eff}(\Delta\tau_5') = \frac{5}{9} T(\Delta\tau_5') + \frac{1}{3} T(p_3 \Delta\tau_5'/p_5) + \frac{1}{9} T(p_1 \Delta\tau_5'/p_5 \qquad (25)$$

The computation is readily carried out by splitting the entire τ_5 interval into m zones and assuming

$$j'(\tau_5') = j_i' = \text{const} \qquad (26)$$

in each zone. Then at the bottom of the i^{th} zone

$$4\pi I_i = \sum_{k=i}^{m} j_k' \Delta W_{ki} \qquad (27)$$

where

$$\Delta W_{ki} = \int_{\tau_k}^{\tau_{k+1}} T_{eff}(\tau_i - \tau')\, d\tau' \qquad (28)$$

By starting at the last zone and working backward the j_i can be obtained in a few moments of hand calculation.

j' is plotted as a function of τ_5 in Fig. 2 and as a function of altitude in Fig. 3. As usual the transformation from τ to z as a variable is made through the relationship

$$j'(z) = \sigma_o p_5 n(z) j'(\tau_5) \quad . \tag{29}$$

Near 200 km j' is of the order of 10^9 excitations per second per cm^2 per unit optical depth and 10^6 excitations per second per cm^3. There is a maximum in the excitation rate per unit optical depth at $\tau_5 = 2350$, corresponding to 203 km but the rate per unit volume rises almost exponentially following the oxygen density down to very low altitude.

To solve the integral equation (23) for the primary excitation rate j_o' in principle is trivial but practically impossible if it is attempted with the equation in the form (23). This is because j_o is very samll compared to j - by a factor of about 10^{-4} - and the difference between the two terms on the right hand side is very small. Furthermore, $H(\tau - \tau')$ varies quite rapidly for small values of $(\tau - \tau')$ and the integration requires that j' be known very accurately near τ. It is for this reason, as we have pointed out in previous papers[2, 3], that it is advantageous to recast this equation so that all terms are of the same order of magnitude. This can be done by making use of the relationship

$$E(\tau) = 1 - \int H(\tau, \tau') \, d\tau' \tag{30}$$

where $E(\tau)$ is the escape probability from the level τ, multiplying through by $j(\tau)$ and adding the resulting equation to (23). The result is

$$j_o'(\tau) = j'(\tau) E(\tau) + \int \left[j'(\tau) - j'(\tau) \right] H(\tau, \tau') \, d\tau' \tag{31}$$

The integrand now goes to zero at $\tau = \tau'$ and where $j'(\tau)$ is increasing or decreasing monotonically, as it does for most values of τ, the positive and negative contributions from small values of $|\tau - \tau'|$ tend to cancel each other and the bulk of the integral comes from the easily evaluated ranges of τ' fairly far from τ.

The function $E(\tau)$ is given by

$$E(\tau) = \mathcal{E}(\tau) + \mathcal{E}(\tau_v - \tau) \qquad (32)$$

where τ_v is the total vertical optical depth to 110 km. $\mathcal{E}(\tau)$ is the probability that a photon emitted somewhere will cross a horizontal plane a distance τ away. Thus

$$H(\tau) = -\frac{\partial \mathcal{E}}{\partial \tau} \qquad (33)$$

These functions have been defined in previous papers[2, 3]. To facilitate computation a brief table of value for $\mathcal{E}(\tau)$ and $H(\tau)$ is presented here

τ	$\mathcal{E}(\tau)$	$H(\tau)$
0	5(-1)	1.27(0)
0.1	3.95(-1)	7.25(-1)
0.5	2.25(-1)	2.61(-1)
1	1.36(-1)	1.19(-1)
10	8.5 (-3)	9.24(-4)
10^2	6.2 (-4)	3.1 (-6)
10^3	4.75(-5)	3.2 (-8)
10^4	4.75(-6)	3.5(-10)
10^5	4.5 (-7)	3.5(-12)

The approximation to j_o' which is $j'E$ is plotted in Fig. 3. It is clear from (31) that j_o' will be larger than $j'E$ near the maximum in $j'(\tau)$ since the integrand is mainly or entirely positive there. There will be two values of τ above and below the maximum where the correction is zero. Beyond these levels - toward the top and bottom of the medium j_o' will be less than $j'E$. The evaluation of the correction integral is readily carried out. (Care again must be taken to use H_{eff} consisting of the weighted contributions from the three lines.) The results for j_o' expressed as a function of 2 and as a function of τ are presented in Figs. 2 and 3. j_o' is a much more sharply peaked function than j' and of course is much smaller. Diffusion of the resonance photons after they are first emitted builds up the level of excitation and spreads it far above and below the region in which the source is concentrated. The maximum in j_o' occurs at 190 km and is only 29 excitations per cm^3 per second. Imprisonment builds up $j'(z)$ to 1.6×10^6 per cm^3 per sec, $j'(z)$ is 8.8×10^6 per cm^3 per second and at 300 km where j_o' is only 2 per cm^3 per sec $j'(z)$ is 5×10^4 per cm^3 per sec.

3. The Forbidden Line at 1356Å.

The forbidden line at 1356Å corresponding to the transition $3s\ ^5S_2 \rightarrow\ ^3P_{2,1}$ is surprisingly strong in the airglow. It has been pointed out that radiative transfer would reproduce the altitude profile of this radiation only if the optical depth were 4 down to 122 km and even then the absolute intensity expected would be two orders of magnitude less than observed[3]. Since the opacity should only be 0.3, scattered solar radiation is inadequate on all counts. Hence the evidence from this

line, even before the Javelin experiment on λ1302-06 was taken to be strongly in favor of the existence of an excitation source in the F_1 region[3]. It is interesting to suppose that the excitation rate j_o' computed for the ^3S level applies also to the ^5S level and compute the altitude profile of the dayglow radiation by simple integration. The expected variation with altitude is shown in Fig. 4. If O_2 absorption is taken to occur with a cross section of 4×10^{-18} cm^2 the intensity would peak at 135 km at 320 R and decrease as shown rapidly to 92 R at 100 km. the experimentally observed curve is also plotted in the figure. The agreement is so close that there seems little reason to suppose that a source j_o' very closely resembling that plotted in Figs. 2 and 3 exists to populate the ^3S and ^5S levels of atomic oxygen. Furthermore, whatever the process it must populate the ^5S with approximately the same efficiency as it does the ^3S level. In fact considering that the measured ratio of excess 1302-06 intensity to 1356 intensity was about 6/.36 or 16.7 rather than 7.3/.36 or 20 used in this paper the evidence is that excitation of the ^5S level is about 1.3 times as efficient as excitation of the ^5S level and decreases somewhat more rapidly with altitude between 140 km and 300 km. Both of these effects are to be expected in the case of excitation by hot photoelectrons[7]. The cross section for excitation of the ^5S level should be sharply peaked above threshold compared to the cross section for excitation of the ^3S level and rise to a higher value. Thus the ^5S level samples a narrow range of energies in the electron energy distribution and its rate of excitation with altitude will vary more rapidly than that of the ^3S level.

4. Lyman α and the Atomic Hydrogen Distribution

At an exospheric temperature of 850° it is to be expected that the hydrogen content of the upper atmosphere will be much greater than it was during a time of higher solar activity. Based on a model of McAfee[8] involving an escape flux and a flux caused by lateral flow at the base of the exosphere fed by diffusive flow below the integral number of atoms to infinity as a function of altitude for this temperature is

Z(km)	cm^{-2}	γ
100	6.7 (13)	13.5
120	4.2 (13)	8.4
200	3.6 (13)	7.2
500	2.7 (13)	5.4
1000	1.8 (13)	3.6
2000	0.9 (13)	1.8

if there are 3×10^7 atoms/cm^3 at 100 km. The cross section for scattering at the center of the Lyman α line is 2×10^{-13} cm^2 at this temperature.

The optical thickness of such a hydrogen distribution may be varied by changing the density at 100 km. The excitation function has been calculated from (8) and (10) for optical thickness from 2 to 100 corresponding to densities from 0.46×10^7 to 2.3×10^8 at 100 km. Then, from (16), the overhead brightness has been computed as a function of altitude. From Fig. 5 in which the theoretical curves are all normalized at 300 km to 1.87 on Fastie's experimental intensity scale it can be seen that the shape of the experimental altitude variation is not inconsistent with the theoretical

profile for τ_v anywhere between about 8 and 20. This range carries us from 4×10^{13} atoms/cm^2 to 10×10^{13} atoms/cm^2 with densities at 100 km ranging from 1.85×10^7 per cm^3 to 4.5×10^7. In particular 3×10^7 atoms/cm^3 and τ_v 13.5 would fit. Since most Lyman α data appear to call for 3×10^7 atoms/cm^3 at 100 km these results would appear to indicate a factor of about 10 increase in hydrogen abundance in the daytime since 1960.

5. Conclusion

The high altitude rocket experiment measuring the variation in intensity of λ1302-06 to 650 km and λ1216 to 1000 km combined with earlier measurements on λ1356 indicate the presence of a source of excitation from 120 to 300 km which produces about 30 $3s\,^3S$ oxygen atoms per cm^2 per sec at 190 km and about 40 $3s\,^5S$ atoms per cm^3 per sec when the sun is 30° above the horizon and the exospheric temperature is 850°. The experiment also indicates that hydrogen is optically thick above 100 km for these conditions.

ACKNOWLEDGEMENTS

This work was supported in part by the National Science Foundation, Atmospheric Sciences Section, and by the National Aeronautics and Space Administration under Contract NASr-179.

REFERENCES

1. A. O. Nier, J. H. Hoffman, C. Y. Johnson, and J. C. Holmes, J. Geophys. Res. 69, 4629 (1964).
2. T. M. Donahue and W. G. Fastie, Space Research IV (Ed. P. Muller). North Holland, Amsterdam (1964).
3. T. M. Donahue, Planet. Space Sci. 13, 871 (1965).
4. R. Tousey, J. D. Purcell, W. E. Austin, D. L. Garrett and K. G. Widing, Space Research IV (Ed. P. Muller). North Holland, Amsterdam (1964).
5. G. Thomas, Private Communication.
6. W. G. Fastie, H. M. Crosswhite and D. F. Heath, J. Geophys. Res. 69, 4129 (1964).
7. A. Dalgarno and A. I. Stewart, Private Communication.
8. J. R. McAfee, Ph.D. Thesis, University of Pittsburgh, 1965.

FIGURE CAPTIONS

Fig. 1 Predicted dayglow 1302-06 brightness from resonance scattering of sunlight as a function of altitude compared to experimental results. Experimental points are scaled upward by an order of magnitude and joined smoothly to previous low altitude profile shown as a solid line.

Fig. 2 Difference between "observed" 1302-04 brightness and the expected contribution from scattering of solar radiation.

Fig. 3 Final excess $^3S_1$ excitation rate $j'(\tau)$, primary rate $j_o'(\tau)$ and the approximate primary rate of j'_E per unit optical depth per cm^2 per second as a function of τ_5 the optical depth in the λ1302 line.

Fig. 4 Final excess $^3S_1$ excitation rate of $j'(z)$ and primary rate $j_o'(z)$ as a function of altitude.

Fig. 5 λ1356 intensity as a function of altitude for a model in which the rate of excitation of the $^5S_2$ level is the same as that of the $^3S_1$ level. The effect of assuming absorption by O_2 with a cross section of 4×10^{-18} cm^2 is shown and compared with the observed profile.

Fig. 6 Lyman α brightness profile expected for an 850° exospheric temperature together with observed brightness. Theoretical curves are normalized at 300 km and labelled as to optical depth down to 100 km and calculated intensity at 900 km. The τ_v=15 profile is also drawn as a dashed curve shifted downward 0.17 kR. The intensity value accompanying the τ_v=2 curve belongs to 760 km.

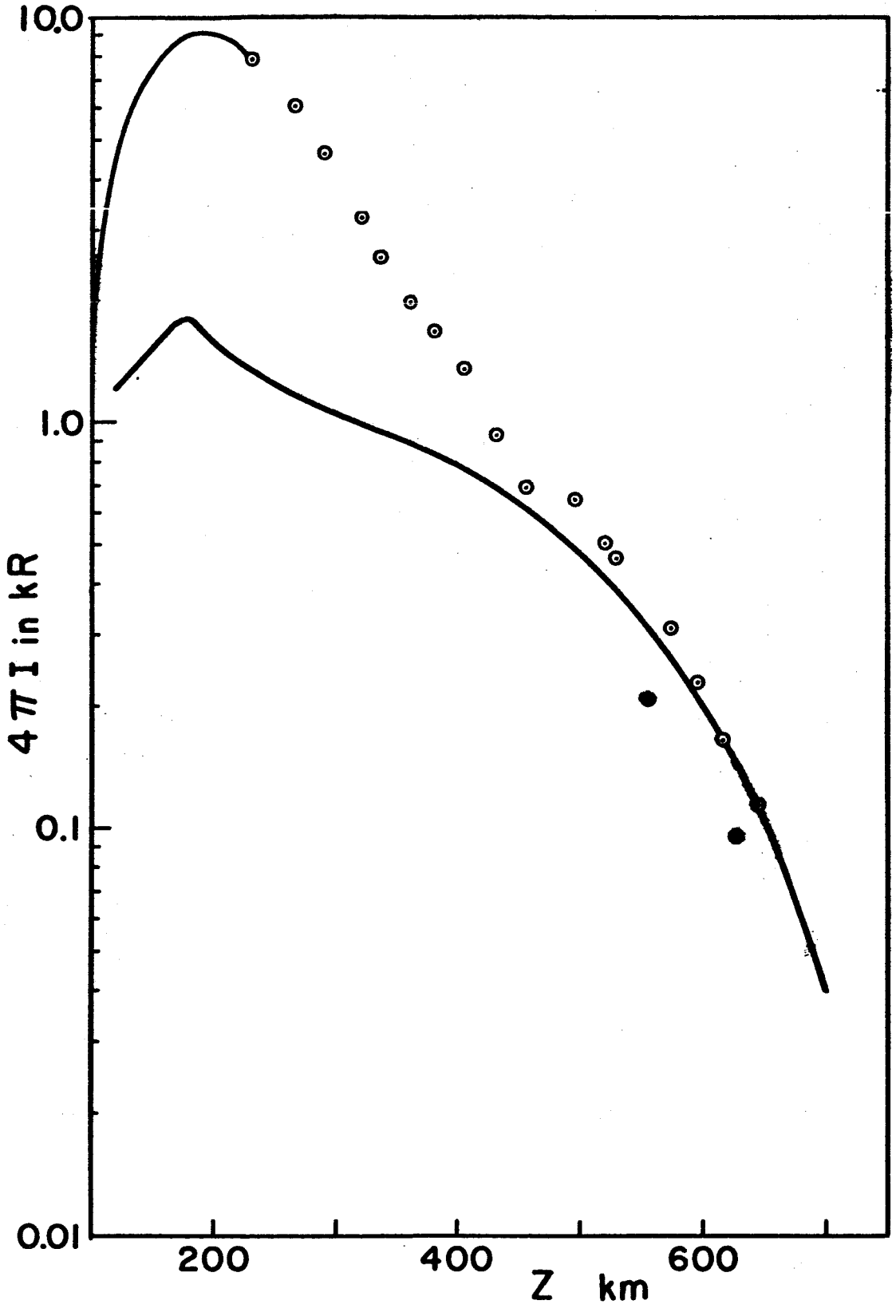

FIG. 1

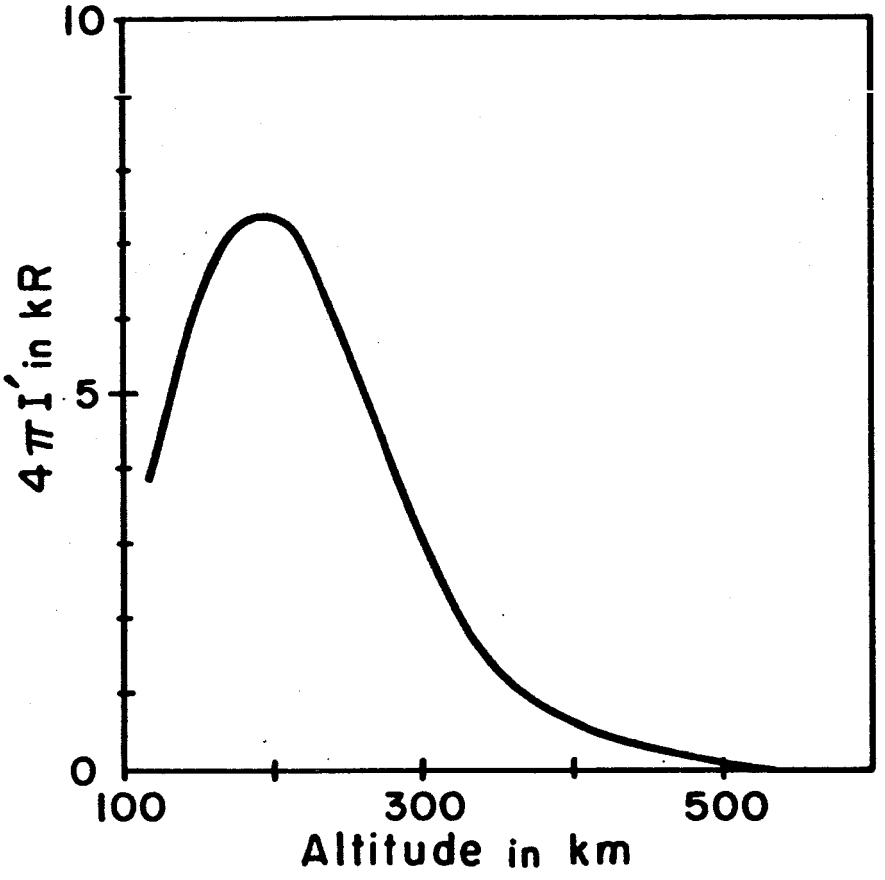

FIG. 2

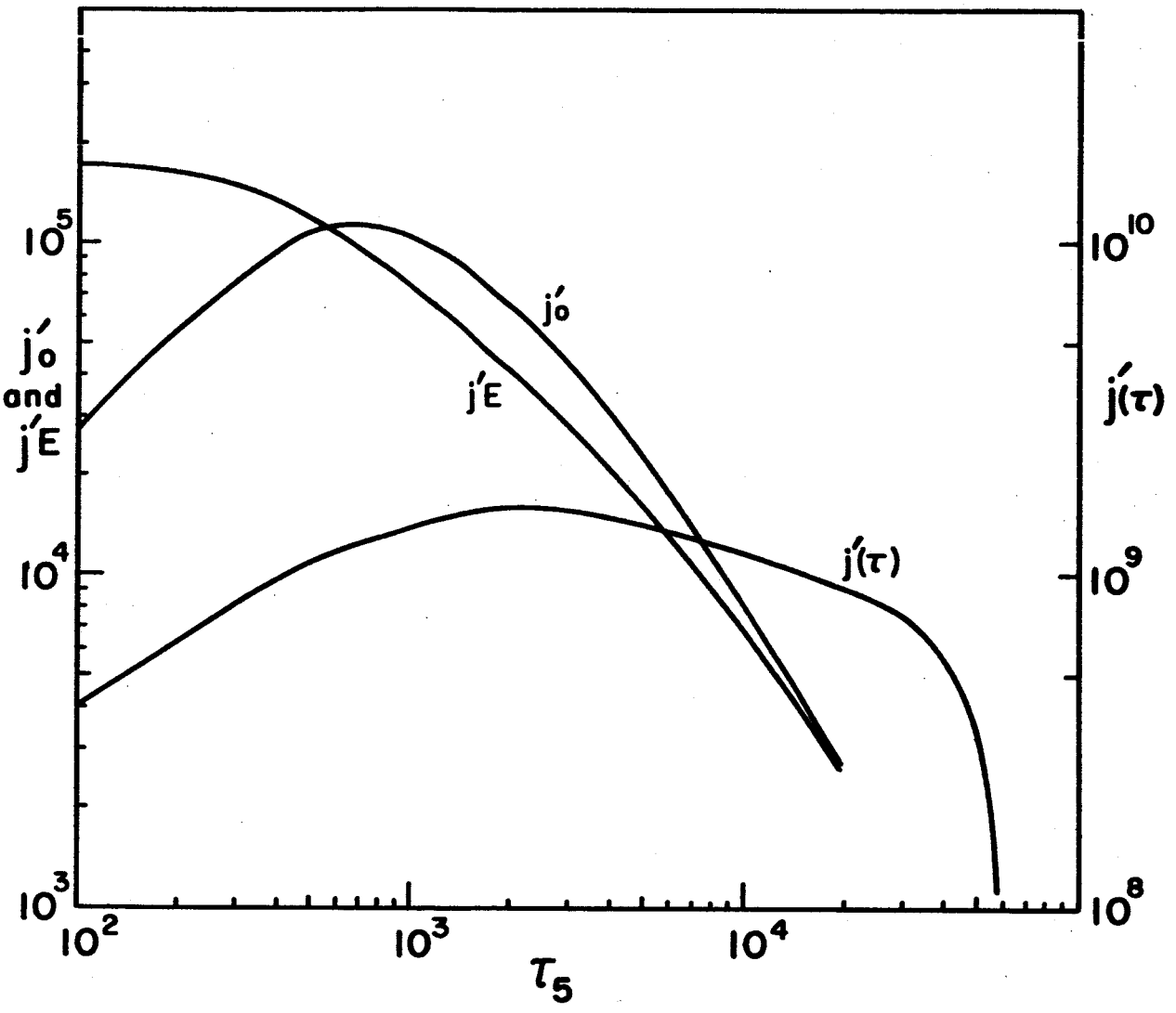
10^5
10^4
10^3
10^{10}
10^9
10^8
j'_o and j'_E
$j'(\tau)$
j'_o
j'_E
$j'(\tau)$
10^2
10^3
10^4
τ_5

FIG. 3

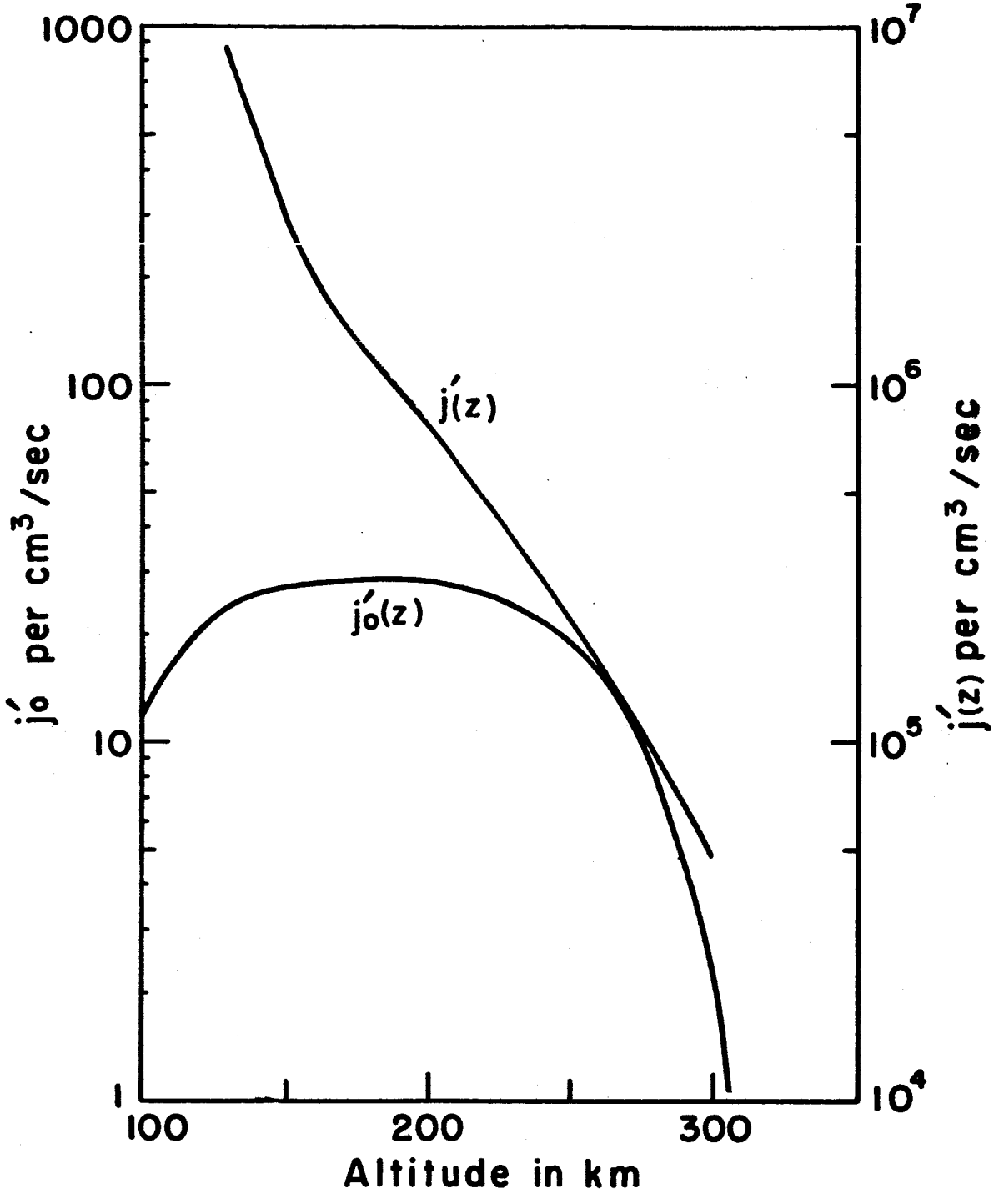
1000
100
10
1
10^7
10^6
10^5
10^4
j'(z)
$j'_o(z)$
j'_o per cm^3/sec
j'(z) per cm^3/sec
100
200
300
Altitude in km

FIG. 4

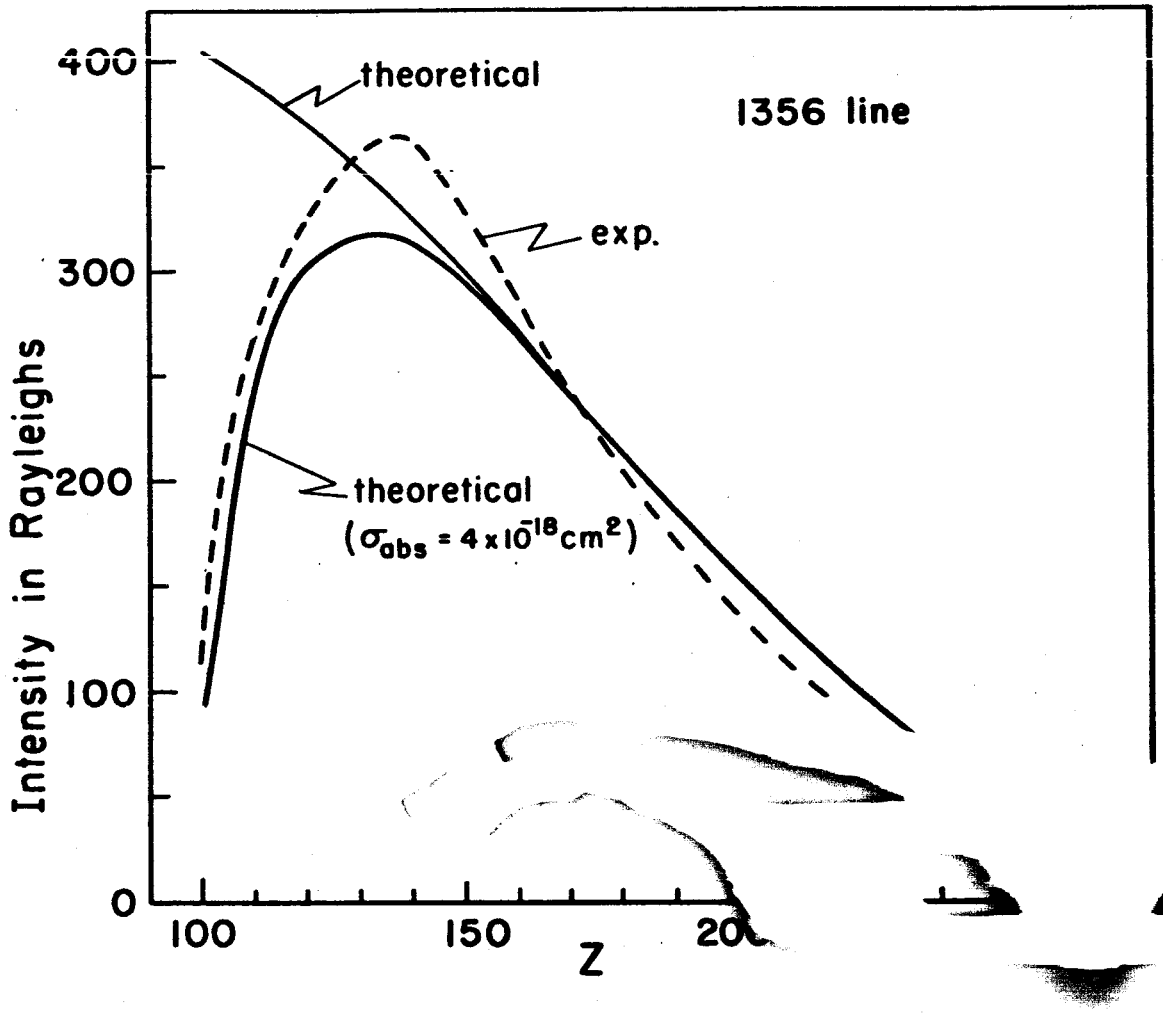
400
300
200
100
0
Intensity in Rayleighs
theoretical
1356 line
exp.
theoretical
($\sigma_{abs} = 4 \times 10^{-18} cm^2$)
100
150
Z

FIG. 5

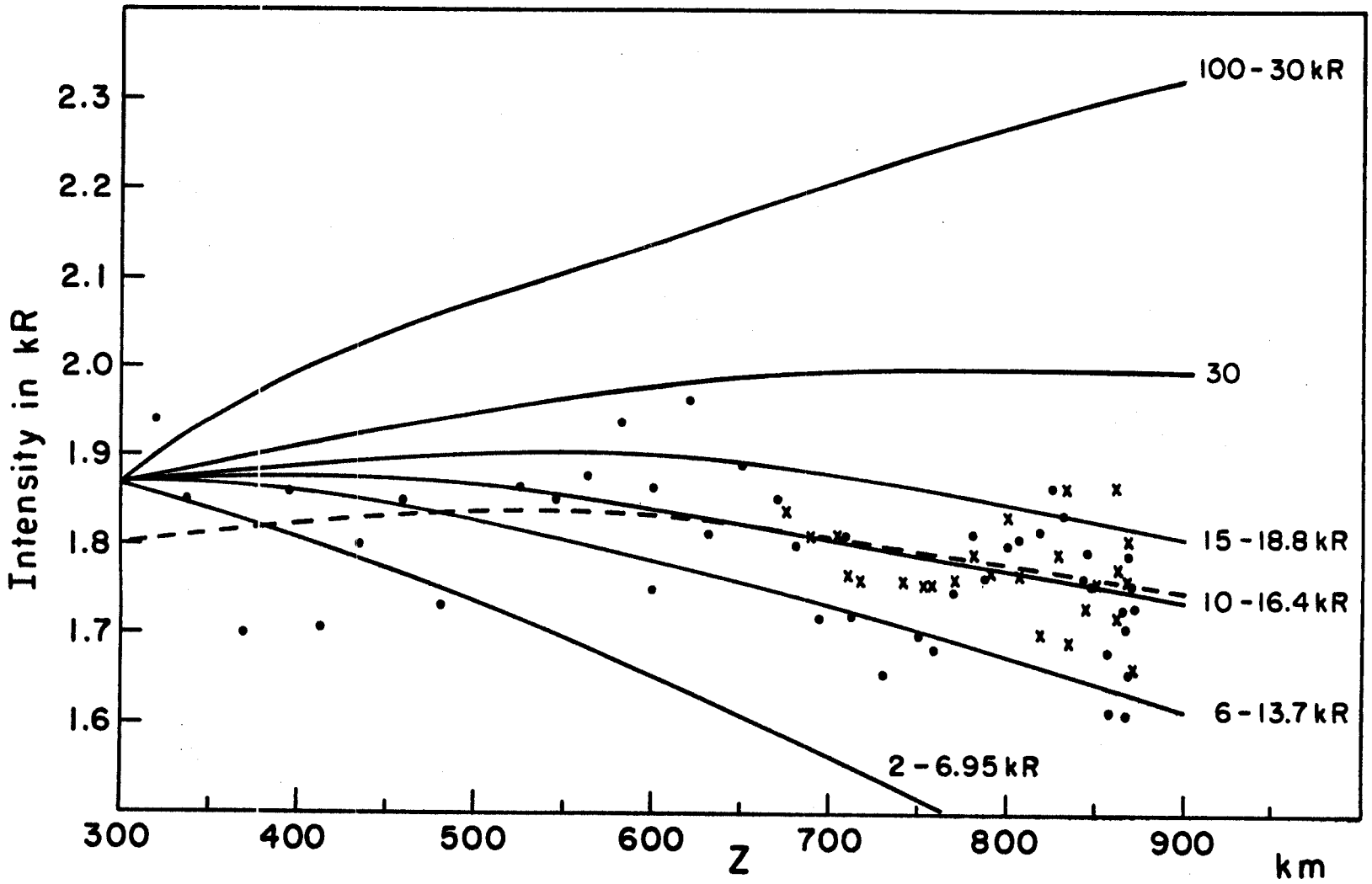
100-30 kR
30
15-18.8 kR
10-16.4 kR
6-13.7 kR
2-6.95 kR
Intensity in kR
2.3
2.2
2.1
2.0
1.9
1.8
1.7
1.6
300
400
500
600
700
800
900
Z
km

FIG. 6